Polymer Testing 93 (2021) 106967

Contents lists available at ScienceDirect

Polymer Testing

journal homepage: http://www.elsevier.com/locate/polytest

Combined roles of temperature and humidity on cure of a silicone elastomer

Matthew T. Elsmore, Davide S.A. De Focatiis *

Faculty of Engineering, University of Nottingham, NG7 2RD, UK

ARTICLE INFO

Keywords:
Cure model
Silicone
Thermal cure
Humidity

ABSTRACT

A study of the cure kinetics of a one-part water-scavenging silicone elastomer was carried out under conditions of controlled humidity and temperature using rectangular bars subjected to oscillatory torsional shear. Characteristic cure times were obtained from Hsich model fits to the storage modulus evolution. A modified Arrhenius-style cure model is proposed that accounts for both the temperature dependence and for the proportionality between rate of cure and concentration of atmospheric water. The 2-parameter model is fitted to a broad dataset and allows accurate predictions of cure times.

1. Introduction

Silicones are widely available in commercial markets, being found in sealants, cooking utensils, sportswear and electrical wiring, and are increasingly used in industrial applications, in particular in the automotive and medical sectors. Silicone sheets and profiles are typically manufactured by calendaring or extrusion processes with a thermally activated cure. Sealant products are instead room-temperature vulcanising (RTV) compounds commonly supplied as a viscous fluid in an applicator. In all cases silicones exhibit a range of useful properties including a low modulus, electrical insulation, hydrophobicity and low toxicity.

Vulcanised silicones are known for their non-stick properties, whereas uncured silicones have very good adhesion and are therefore challenging to shape and handle, making in-situ shaping challenging. With a view to address this, a novel composition of RTV silicone was developed in 2007 by FormFormForm, and marketed under the trade name of Sugru® for commercial DIY markets, and as Formerol® F10 for industrial applications [1]. Both compositions are filled such that the pre-cured state is one of a ductile solid rather than a viscous fluid, and that the adhesion is more limited, thus enabling easier in-situ shaping.

Silicones and polysilazanes are examples of one-part cure systems which do not require manual addition of further chemical constituents in order to initiate cure. RTV silicone sealants, including Formerol® F10, cure at ambient temperature by diffusion of water molecules from the local environment into the material, forming siloxane (Si–O–Si) bonds between the polymer chains [2]. The hydrosilylation reaction is catalysed by platinum, with condensation or addition polymerisation mechanisms generating the resultant cross-linked structure [3]. Polysilazanes cure via a condensation reaction catalysed by amines and ammonia [4], and, similarly to silicones, cross-link via a hydrolysis reaction forming siloxane bonds [5].

Temperature and atmospheric humidity have been shown to play a significant role in the rate at which moisture-scavenging polymers cure. Halasz and Belina conducted experiments to investigate the effect of temperature and molar ratio on cure rate for epoxy powder coatings. Differential scanning calorimetry (DSC) and parallel plate oscillatory rheology were employed to measure isothermal cure progression and the sol-gel transition respectively. Temperature was shown to have a significant impact on gel time, reducing cure times by almost 50% between 160 and 200 °C, with an activation enthalpy, ΔH, of ~65 kJ mol^{-1} [6]. Hong and Lee also used DSC to show the effect of temperature on polydimethylsiloxane (PDMS) cure rates, establishing a ΔH of 106 kJ mol^{-1} [7].

A study conducted by Comyn investigated the effect of moisture absorption and exposure time on cure depth for silicone sealants and other adhesives in single-lap joint configurations on aluminium substrates. Using a series of saturated salt solutions to control humidity within a closed chamber, an increase in relative humidity (RH) from 32.7% to 100% reduced the cure time by ~ 80% for ~3 mm cure depth [8].

A similar study was conducted by De Buyl and co-workers using alkoxysilicone sealants, where cure depth was measured in tubs of depth 7, 11, 17 and 48 mm under varied temperature (5, 25 and 35 °C) and

* Corresponding author.,
E-mail address: davide.defocatiis@nottingham.ac.uk (D.S.A. De Focatiis).

https://doi.org/10.1016/j.polymertesting.2020.106967
Received 30 April 2020; Received in revised form 19 August 2020; Accepted 17 November 2020
Available online 20 November 2020

relative humidity (75.4% and 100% RH) conditions. It was shown that increasing either temperature, humidity or both, resulted in a faster rate of cure and cure depth achieved. Plots of cure depth as a function of the square root of time showed a 'kink' in the experimental data, transitioning to a steeper slope. This indicates presence of an inner and outer region of cure, with the outer region experiencing a greater crosslink density due to a shorter diffusion path for moisture [9].

Raghavan and co-workers showed that for chlorobutyl elastomer systems, which similarly demonstrate crosslinking behaviour during cure, shear storage modulus G' measured in torsion at constant frequency can be used to evaluate cure progression [10]. As time elapsed, G' increased from gelation up to a final value, at which point complete cure is achieved, going by the relationship between shear modulus G and number density of crosslinks within a polymer network N, given by [11].

$$G = Nk_BT \tag{1}$$

where k_B is Boltzmann's constant and T is absolute temperature.

Xie and co-workers also used dynamic mechanical analysis (DMA) in single-cantilever mode to assess cure progression for epoxy pre-impregnated glass fibre networks [12]. Isothermal flexural tests at constant frequency and strain amplitude showed flexural modulus to provide a measure of cure with elapsing time.

The purpose of this study is to provide a more thorough understanding of the cure kinetics of one-part water-scavenging silicone elastomers. Cure progression was measured via the shear modulus as a function of time under conditions of controlled temperature and humidity, and simple cure models were fitted to the data to obtain characteristic cure timescales. This study proposes a combined temperature and humidity model for predicting cure timescales as a function of these quantities.

2. Materials and Methods

2.1. Materials

The material used in these investigations is a one-part RTV silicone elastomer named Formerol F.10 (tradename: *Sugru*). This particular silicone elastomer was selected for study due to several factors that make it suitable for analysis: (1) a sufficiently long shaping time prior to gelling; (2) reasonably short cure timescales at or close to room temperature and humidity, and (3) a sufficiently high viscosity prior to cure such that specimens can be easily formed and maintain their shape during handling. Formerol F.10 cures via condensation and hydrolysis reactions, where moisture from the environment acts as the catalyst to the formation of hydroxyl groups, as shown in Fig. 1 [13]. As cure progresses, the reactive species [S] are depleted and a cross-linked structure is formed. The silane cross-linker used in this reaction also combines as an adhesion promoter to encourage surface adhesion with substrates [14]. Talc and silica-based reinforcing fillers comprise between 3–66% and 10–60% of the total composition respectively, giving the resultant durability and toughness of the material [1].

The reaction kinetics can be approximated by [15].

$$\frac{\partial[S]}{\partial t} = -k(T)\cdot[S]\cdot[H_2O] \tag{2}$$

where $[H_2O]$ is the concentration of water and $k(T)$ is an Arrhenius-dependent rate constant such that

$$k(T) \propto \exp\left(-\frac{\Delta H}{RT}\right) \tag{3}$$

where R is the gas constant.

The material is supplied in sealed packets that prevent moisture entry, and is designed to be moulded into shape within ~30 min, after which time cure takes place in ~1 day under standard UK atmospheric conditions (~21 °C and 50% RH), forming a tough, durable rubber [16]. For the purpose of this investigation, sheets of white Formerol F.10 were manually pressed to a thickness of 3.3 mm using a custom-made mould, and rectangular bars 4.5 mm in width and ~25 mm long were cut using a parallel-sided blade jig.

2.2. Measurement conditions and procedure

In order to study the progression of cure under controlled conditions, an Anton Paar MCR302 rheometer fitted with a CTD450 environmental chamber and torsional bar grips is used. For humidity control, the chamber is sealed and fed by a Linkam RH95 humidity controller. The temperature control is achieved by a temperature-regulated water recirculator connected to the shell of the chamber, and air access to the chamber is limited only to the narrow gap between the drive shaft and the chamber. An independent DHT22 humidity sensor is fixed inside the chamber and coupled to an Arduino UNO for temperature and humidity data collection.

Bar specimens were clamped and allowed to acclimatise, after which time an oscillatory shear strain of 1% was applied at a fixed frequency of 1 Hz. The elastic, in-phase part of the shear modulus $G'(t)$ was determined from the torque response as an indicator of cure progression χ at time t, since for an elastomeric network this is proportional to the crosslink density [17]. In order to obtain a characteristic cure timescale τ at a given temperature and humidity, a Hsich model was fitted to each experiment, given by [18].

$$\frac{G'_\infty - G'(t)}{G'_\infty - G'_0} = \exp\left[-\left(\frac{t}{\tau}\right)\right] = 1 - \chi \tag{4}$$

where G'_0 and G'_∞ are the moduli at the start and end of cure respectively. In all cases, the Hsich model was fitted to data after the gel point crossover had been achieved, using a least squares error approach.

A range of temperature between 20 and 40 °C, and of absolute humidity between 3.4 and 22.1 g m^{-3} was explored. The chamber acclimatises in ~30 min, and each test was carried out for up to 72 h, during which time the variations in temperature and humidity were of the order of ±2 °C and ranged between ±0.1–2.2 g m^{-3} depending on the applied conditions. A total of 22 experiments were carried out to measure temperature and humidity dependence.

Maintaining a specific relative humidity throughout experiments of such long duration represented the largest source of error during these investigations. Measured humidity trends throughout experiments showed a sinusoidal fluctuation around the desired relative humidity, deviating by amplitudes of up to ±10% RH. Higher temperature tests

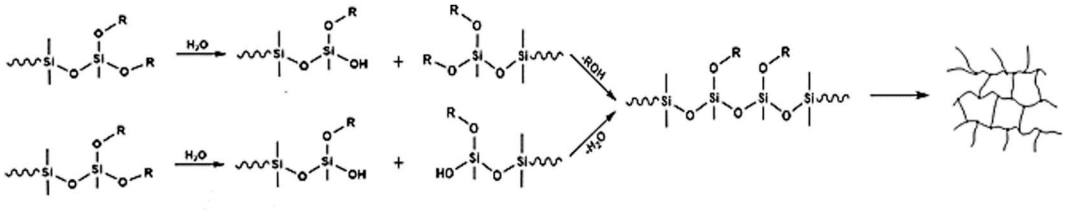

Fig. 1. The basic mechanisms of hydrolysis and condensation of Formerol F.10 that lead to the formation of a cross-linked rubber network, adapted from [13].

(~40 °C) led to the worst humidity control, likely due to the increased supply rate for moisture required by the system to achieve the required relative humidity. Temperature control via the water circulation system was more reliable, with minimal variation in temperature in the chamber, and no test exceeding a standard deviation of ±0.9 °C from the mean. Fig. 2 shows the experimental configuration for humidity and temperature controlled rheometry, the bar torsion clamping arrangement and typical cure atmosphere data as recorded by the independent Arduino DHT22 sensor in parts (a), (b) and (c) respectively.

To confirm reproducibility of the experimental results, three repeats were conducted at (18.9 ± 1.5) °C and (48.5 ± 3.4)% RH. Whilst the values of G'_∞ ranged between 9.7 MPa and 12.7 MPa, the values of τ varied only between 11.4 and 12.3 h. This suggests that the experiment is appropriate in obtaining reproducible values of τ despite some observed discrepancies in the final state of the material. Due to the limited quantity of available material, no further repeat testing was conducted for other experimental conditions.

3. Results

3.1. The role of temperature on cure

In order to study the effect of temperature on cure, a series of tests were performed in which temperature was varied but absolute humidity, i.e. $[H_2O]$, was kept as constant as possible. In order to convert relative humidity to absolute humidity, the AERK Magnus formulation for saturation vapour pressure as a function of absolute temperature $e_w(T)$ is employed [19].

$$e_w(T) = 6.1094 \exp\left(\frac{17.625T - 4814.27}{T - 30.11}\right) \quad (5)$$

Thus, $[H_2O]$ can be written as [7].

$$[H_2O] = \frac{2.16679 e_w(T)}{T} \cdot RH \quad (6)$$

A value of absolute humidity $[H_2O] = (4.7 \pm 0.7)$ g m^{-3} was selected as it enabled relative humidity values to be set in a range suitable for the humidity controller across a target temperature range of 20–40 °C. Experimental measurements of cure using bars in torsion were carried out in this temperature range, at 5 °C intervals, and Hsich models, and hence τ values, were obtained for each test. Test and model parameters are given in Table 1.

The Hsich model produces excellent representations of the cure data across the range of conditions explored, with $R^2 > 0.998$. Representative cure data sets and fitted Hsich models under conditions of approximately constant absolute humidity are shown in Fig. 3.

An increase in temperature from 19.3 °C to 39.2 °C leads to an approximate halving of the cure timescale τ. There are larger variations

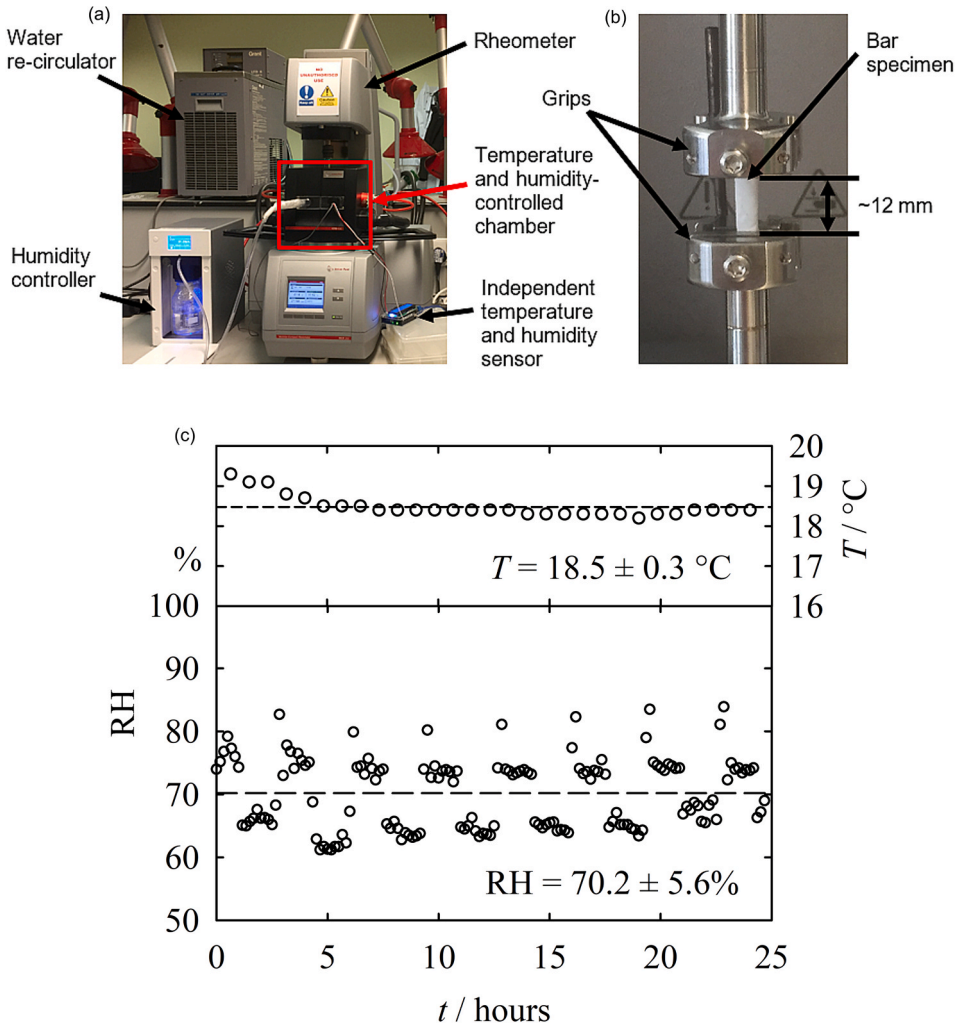

Fig. 2. (a) Experimental configuration for controlled humidity and temperature, (b) bar torsion clamping arrangement, and (c) typical temperature (right abscissa) and relative humidity (left abscissa) logs produced during experiments, showing a good level of temperature control but larger fluctuations in humidity. Mean values for temperature and relative humidity over the experiment duration are given by dashed lines.

Table 1
Approximately constant absolute humidity test conditions employed to explore the temperature dependence of cure, with Hsich cure model parameters fitted to each experiment. ± denotes one standard deviation for test conditions and one standard error for model parameters.

T (°C)	RH (%)	[H_2O] (g m^{-3})	$G_\infty^{'}$ (MPa)	τ (hours)
19.3 ± 0.1	29.8 ± 0.7	5.2 ± 0.1	9.15 ± 0.01	21.77 ± 0.04
24.6 ± 0.1	19.8 ± 1.4	4.5 ± 0.3	16.5 ± 0.02	19.3 ± 0.06
29.9 ± 0.2	17.2 ± 1.4	5.2 ± 0.4	10.74 ± 0.01	15.51 ± 0.04
33.9 ± 0.4	13.3 ± 2.4	4.9 ± 0.9	18.06 ± 0.02	15.10 ± 0.05
39.2 ± 0.3	7.6 ± 1.9	3.9 ± 1.0	10.71 ± 0.01	11.05 ± 0.02

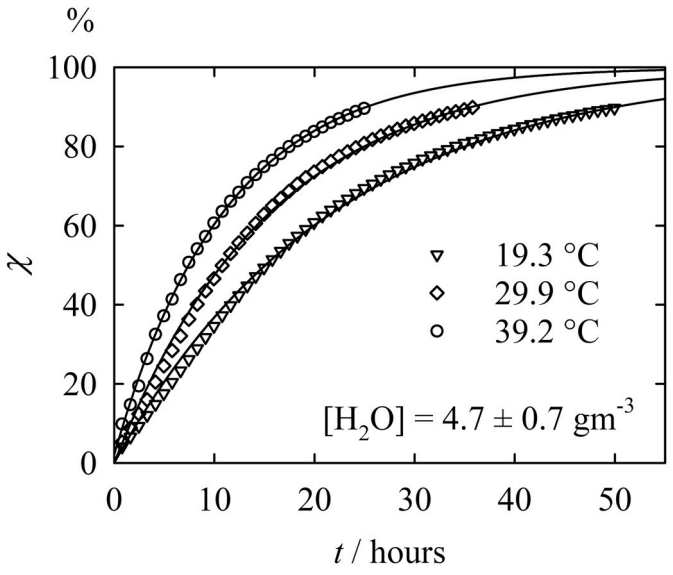

Fig. 3. Cure progression for three temperatures as a function of cure time, illustrating the effect of temperature under conditions of approximately constant humidity [H_2O] = (4.7 ± 0.7) g m^{-3} (±one standard deviation). Corresponding Hsich model fits shown as solid lines.

in $G_\infty^{'}$, which may be attributed to the challenges in achieving regular, uniform bar cross-sections, particularly in the regions in the vicinity of the clamps.

An Arrhenius plot is generated to explore the temperature dependence of the cure timescale and is shown in Fig. 4. The data shows Arrhenius behaviour and relaxation times can be expressed as

$$\tau = \tau^* a_T \quad \text{where} \quad a_T = \exp\left[\frac{\Delta H}{R}\left(\frac{1}{T} - \frac{1}{T^*}\right)\right] \tag{7}$$

and τ^* is a characteristic cure time at reference temperature T^*. Setting T^* = 292.1 K (18.9 °C) and carrying out linear regression produces an activation enthalpy ΔH = (24.8 ± 5.2) kJ mol^{-1} with τ^* = (22.8 ± 2.0) hours, where ± denotes one standard error.

3.2. The role of humidity on cure

From the reaction chemistry, it is postulated that rates of cure should be proportional to the concentration of water. The effect of humidity at a constant temperature of T = (38.9 ± 0.3) °C = (312.1 ± 0.3) K is illustrated in the results presented in Table 2 and Fig. 5, and shows a reduction in τ from ~11 to ~4 h as humidity increases from 7.6% to 36.7% RH. The availability of atmospheric moisture in the form of humidity therefore has a significant impact upon curing rate, in the same manner as was found by Comyn for fluorosilicone sealant cure [8].

In order to isolate the effect of humidity from that of temperature, cure times established by Hsich model fits were normalised with respect

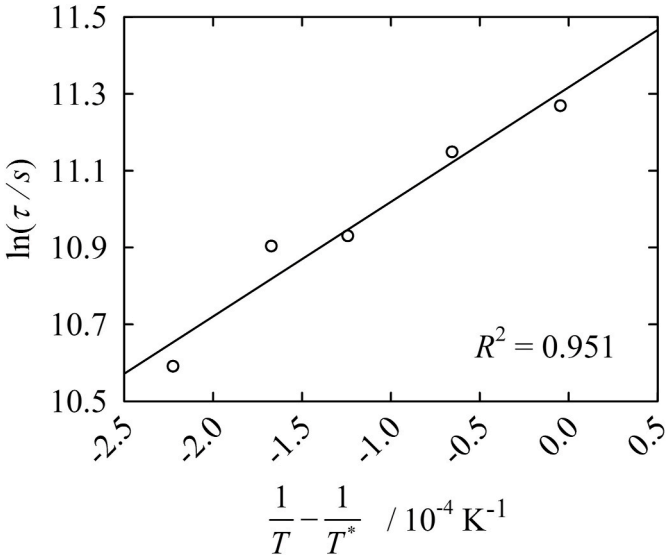

Fig. 4. Arrhenius plot of cure timescales at various temperatures, with linear regression showing ΔH = (24.8 ± 5.2) kJ mol^{-1}. Reference temperature T^* = 292.1 K.

Table 2
Approximately constant temperature test conditions employed to explore the effect of humidity on cure, with Hsich cure model parameters fitted to each experiment. ± denotes one standard deviation for test conditions and one standard error for model parameters.

T (°C)	RH (%)	[H_2O] (g m^{-3})	G_∞ (MPa)	τ (hours)
39.2 ± 0.3	7.6 ± 1.9	3.9 ± 1.0	10.71 ± 0.01	11.05 ± 0.02
38.9 ± 0.3	18.1 ± 0.8	9.2 ± 0.4	10.73 ± 0.01	6.78 ± 0.02
38.9 ± 0.1	28.5 ± 2.0	14.6 ± 1.0	9.63 ± 0.01	4.79 ± 0.01
40.6 ± 0.2	36.7 ± 5.2	18.8 ± 2.6	10.22 ± 0.01	3.91 ± 0.01

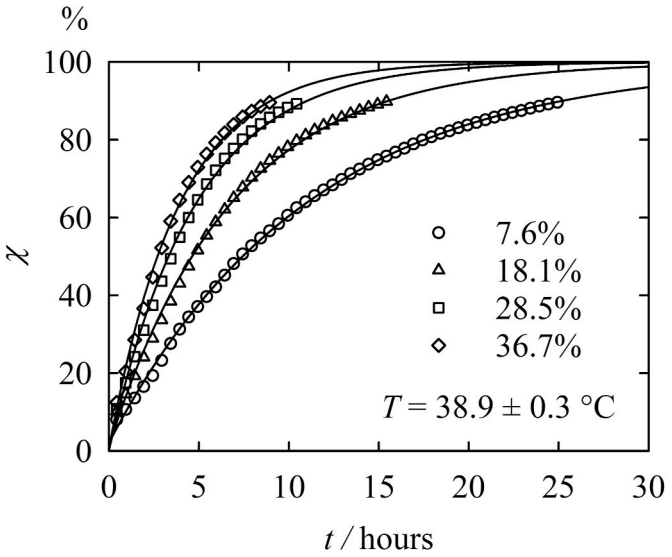

Fig. 5. Cure progression for four relative humidities as a function of time at constant temperature T = (38.9 ± 0.3) °C (±one standard deviation). Corresponding Hsich model fits shown as solid lines.

to the reference value (obtained at a nominally fixed absolute humidity of [H_2O] = (4.7 ± 0.7) g m^{-3}) shifted to the equivalent temperature obtained from the Arrhenius equation, and the normalised quantity $\tau/\tau^* a_T$ is plotted as a function of the inverse of the normalised absolute

humidity $[H_2O]/[H_2O]^*$ in Fig. 6. This is done since it is expected that the cure rate should be proportional to the absolute humidity, and hence the cure time should be inversely proportional to the same quantity. Here reference temperature and humidity values of $T^* = 292.1$ K (18.9 °C), $[H_2O]^* = 7.85$ g m^{-3} and $\tau^* = 12.2$ hours are used as obtained from the repeatability study. The gradient of the line was found to be 1.05 ± 0.04. This is sufficiently close to unity for the purpose of the estimation of cure times.

3.3. A combined temperature and humidity model

A combined expression for the effects of temperature and humidity on characteristic cure times can be formulated by adding a further humidity shift factor a_H to the Arrhenius expression presented in eq. (7) as

$$\tau = \tau^* a_T a_H \tag{8}$$

where a_H is expressed as

$$a_H = \left(\frac{[H_2O]^*}{[H_2O]}\right) \tag{9}$$

In order to make use of all of the experiments carried out at a wider range of temperatures and humidities, a simultaneous least-squares fitting of the model constants τ^* and ΔH was carried out on the entire dataset. This exercise determined values of $\tau^* = (11.9 \pm 0.7)$ hours and $\Delta H = (28.8 \pm 4.0)$ kJ mol^{-1} at reference conditions of $T^* = 20$ °C and 50% relative humidity (i.e. $[H_20]^* = 8.63$ g m^{-3}), with a correlation coefficient of $R^2 = 0.885$.

4. Discussion

4.1. Determination of cure times

The model and parameters allow the plotting of reference graphs for the simple determination of cure times at a range of temperatures and relative humidities of interest. Fig. 7 shows τ values generated by the model as a function of temperature for various humidities, and Fig. 8 as a function of humidity for various temperatures. The values of τ refer to the characteristic time constants of the cure reaction, and hence to determine practical cure times one should consider the extent to which the cure reaction is completed. For example, after τ one can expect to have reached ~63% of the final stiffness, and this increases to 95% after

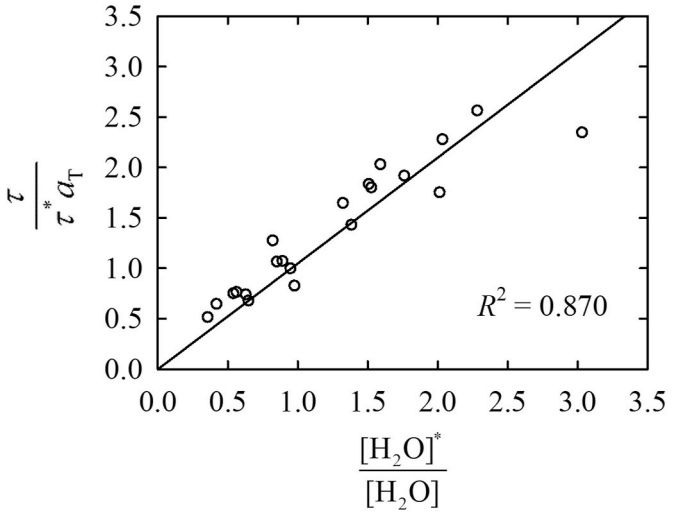

Fig. 6. Temperature-normalised cure times as a function of the inverse of the normalised absolute humidity, demonstrating the proportionality between rate of cure and absolute humidity. Reference conditions of $T^* = 292.1$ K (18.9 °C), $[H_2O]^* = 7.85$ g m^{-3} and $\tau^* = 12.2$ hours .

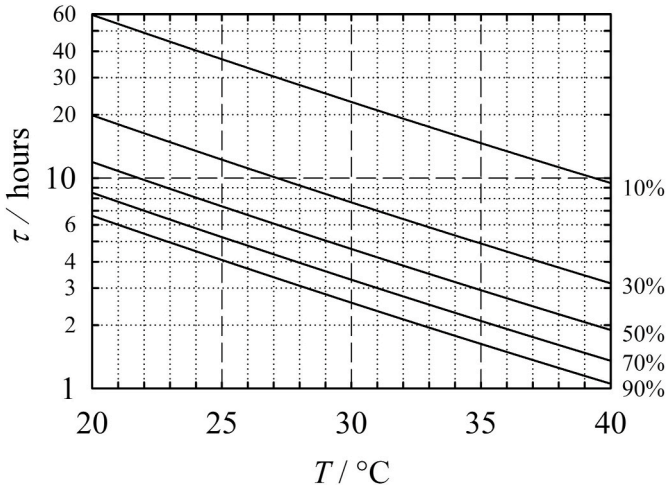

Fig. 7. Cure timescale as a function of temperature for relative humidity values between 10 and 90% in 20% intervals as predicted by the model.

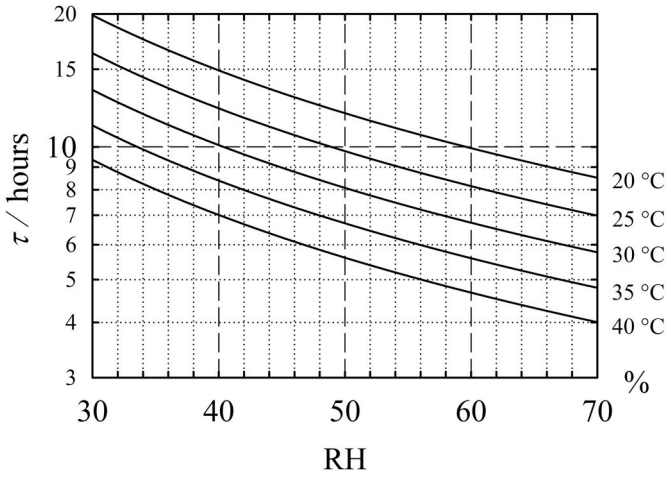

Fig. 8. Cure timescale as a function of relative humidity for temperatures between 20 and 40 °C in 5 °C intervals. Increasing moisture concentration produces an exponential reduction in predicted τ at all reference temperatures.

3τ, and to 99% after 5τ. At a typical ambient temperature of 21 °C and 50% RH a value of τ of 10.81 h is produced; when considering the recommended cure time at the same conditions of 24 h found on the manufacturer's data sheet [16], it suggests that around 2.5τ are needed, and that the recommended level of cure for practical applications is ~92%.

4.2. Consideration of thickness effects

Experimental measurements shown thus far have been carried out at a fixed sample thickness of 3.3 mm, and hence the diffusion pathway for water has been 1.65 mm. This has enabled the condition for diffusion timescales to be considerably shorter than the cure timescales, and hence that the concentration of water in the specimen remains in equilibrium at the same concentration as the environment. Attempts to measure a saturation water concentration in both uncured and fully cured specimens did not yield measurable quantities, probably due to the relatively high hydrophobicity of silicone.

A small subset of cure measurements were carried out on specimens with varying thickness from 1.93 to 4.66 mm at fixed $T = (19.8 \pm 0.5)$ °C and $[H_2O] = (8.6 \pm 0.6)$ g m^{-3}. The cure progressions are illustrated as a function of time together with Hsich model fits in Fig. 9. There is a small

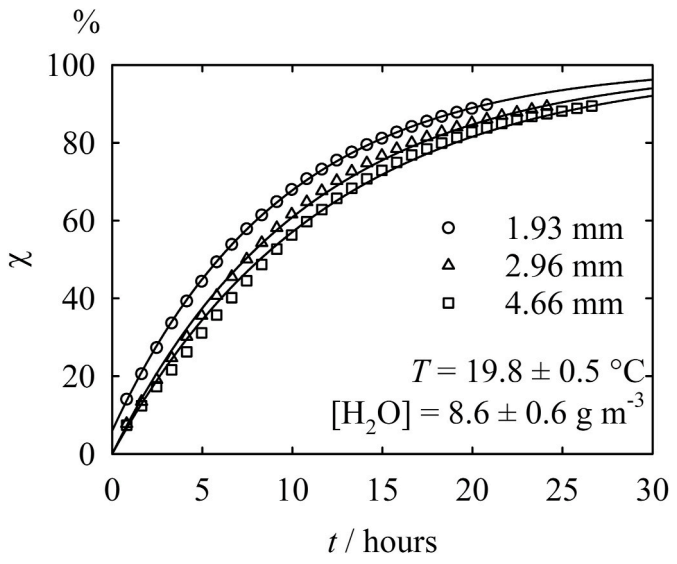

Fig. 9. Cure progression of samples of different thickness at fixed T = (19.8 ± 0.5) °C and [H2O] = (8.6 ± 0.6) g m−3 (symbols). Hsich model fits are shown as lines.

increase in the cure timescale as the thickness is increased, from 9.3 to 11.3 h across the range, suggesting that there is a partial thickness effect. Consistent with Comyn and De Buyl's observations for sealants and adhesives, this is primarily attributed to the effect of the cure of the outer skin on the diffusion of water [8,9]. Additionally, the geometry of the specimen is such that outer skin dominates the torsional stiffness relative to the interior since both the contribution to the polar second moment of area and the shear strains are larger the further away material is from the axis of rotation. A different mode of deformation such as tension would eliminate this effect.

Although it is acknowledged that diffusion and skin effects may present a greater challenge in curing particularly thick components, for the general intended applications of this material the effects of thickness can be considered small.

5. Conclusions

By coupling a humidity controller to a rotational rheometer, the curing behaviour of Formerol F.10 silicone elastomer bars was monitored in torsional oscillatory shear under conditions of controlled temperature and humidity. Characteristic cure timescales were estimated by fitting the storage modulus vs time curves to a Hsich model for each experiment.

A cure model is proposed that follows Arrhenius temperature dependence and a proportionality between the cure rate and the absolute humidity, and it was shown that the model is able to provide a good fit to the broad dataset ($R^2 = 0.885$). The model is useful in estimating the degree of cure of Formerol F.10 under practical variations of ambient temperature and humidity, and for specimens with diffusion length scales of a few mm.

Declaration of competing interest

The authors declare that they have no known competing financial interests or personal relationships that could have appeared to influence the work reported in this paper.

Acknowledgements

The authors acknowledge the contributions of FormFormForm Ltd for the supply of the raw materials, and of Tom Dowden, Paraskevi Christogianni and Harry Alexander for helpful discussions on the experiments. This research did not receive any specific grant from funding agencies in the public, commercial, or not-for-profit sectors.

Appendix A. Supplementary data

Supplementary data to this article can be found online at https://doi.org/10.1016/j.polymertesting.2020.106967.

References

[1] J.M. Delehanty, I. Moss, S. Westall, Mouldable One-Part RTV Silicone Elastomer, GB2444255, 2006.
[2] Dow Corning Corporation, A Guide to Silane Solutions: the Basics of Silane Chemistry, 2009.
[3] J.K. Fink, Terpene Resins, in *Reactive Polymers Fundamentals and Applications*, William Andrew Publishing, 2013.
[4] S. Marceaux, C. Bressy, F.-X. Perrin, C. Martin, A. Margaillan, Progress in Organic Coatings Development of polyorganosilazane – silicone marine coatings, Prog. Org. Coating 77 (2014) 1919–1928.
[5] A.J. Müller, R.M. Michell, Differential Scanning Calorimetry of Polymers, in Polymer *Morphology : Principles, Characterization, and Processing*, John Wiley & Sons Inc., 2016.
[6] L. Halasz, K. Belina, An investigation into the curing of epoxy powder coating systems, J. Therm. Anal. Calorim. 119 (2015) 1971–1980.
[7] I. Hong, S. Lee, Cure kinetics and modeling the reaction of silicone rubber, J. Ind. Eng. Chem. 19 (2013) 42–47.
[8] J. Comyn, Moisture cure of adhesives and sealants, Int. J. Adhesion Adhes. 18 (1998) 247–253.
[9] F. De Buyl, J. Comyn, N.E. Shephard, N.P. Subramaniam, Kinetics of cure, cross link density and adhesion of water-reactive alkoxysilicone sealants, J. Adhes. Sci. Technol. 16 (8) (2002) 1055–1071.
[10] S.R. Raghavan, L.A. Chen, C. McDowell, S.A. Khan, R. Hwang, S. White, Rheological study of crosslinking and gelation in chlorobutyl elastomer systems, Polymer (Guildf). 37 (26) (1996) 5869–5875.
[11] G. Rehage, Elastic properties of crosslinked polymers, Macromol. Chem. (1973) 161–178.
[12] M. Xie, Z. Zhang, Y. Gu, M. Li, Y. Su, A new method to characterize the cure state of epoxy prepreg by dynamic mechanical analysis, Thermochim. Acta 487 (2009) 8–17.
[13] K. Nguyen, Silicone Cross-Linking Chemistries: from Kinetics to Dynamics of Mechanical Properties for Biomedical Applications, " Queen Mary University of London, 2017.
[14] W.D. Bascom, Structure of silane adhesion promoter films on glass and metal surfaces, Macromolecules 5 (6) (1970) 792–798.
[15] S. Kumar, S.K. Samal, S. Mohanty, S.K. Nayak, Study of curing kinetics of anhydride cured petroleum-based (DGEBA) epoxy resin and renewable resource based epoxidized soybean oil (ESO) systems catalyzed by 2-methylimidazole, Thermochim. Acta 654 (2017) 112–120.
[16] FormFormForm Ltd, Let's Get Technical, 2016, pp. 1–12.
[17] L.R.G. Treloar, The elasticity and related properties of rubbers, Rep. Prog. Phys. 36 (7) (1973) 755–826.
[18] H.S.Y. Hsich, Kinetic model of cure reaction and filler effect, J. Appl. Polym. Sci. 27 (9) (1982) 3265–3277.
[19] O.A. Alduchov, R.E. Eskridge, Improved Magnus form approximation of saturation vapour pressure, J. Appl. Meteorol. 35 (1995) 601–609.